Evidence of three-dimensional Ising ferromagnetism in the A-site-ordered perovskite CaCu_{3}Ge_{4}O_{12}

J.-G. Cheng, J.-S. Zhou, J. B. Goodenough, Y. T. Su, and Y. Sui

Phys. Rev. B **83**, 212403 — Published 23 June 2011

DOI: 10.1103/PhysRevB.83.212403

Evidence of 3D Ising ferromagnetism in the A-site ordered perovskite $CaCu_3Ge_4O_{12}$

J.-G. Cheng, J.-S. Zhou, and J. B. Goodenough

Materials Science and Engineering Program/Mechanical Engineering, University of Texas at Austin, Austin, TX 78712, USA

Y. T. Su, and Y. Sui

Center for Condensed Matter Science and Technology, Department of Physics, Harbin Institute of Technology, Harbin, 150001, China

Abstract

The A-site-ordered perovskite $CaCu_3Ge_4O_{12}$ synthesized under high pressure undergoes ferromagnetic spin ordering below $T_c \approx 12$ K. The critical exponents have been determined from isotherms of magnetization across T_c via an iteration process and the Kouvel-Fisher method as well as from specific heat. Based on fitting parameters of T_c, β and γ, the magnetization data in the vicinity of T_c can be scaled onto two universal curves in the plot of $M/|\varepsilon|^{\beta}$ versus $H/|\varepsilon|^{\beta+\gamma}$, where $\varepsilon = T/T_c-1$. Critical exponents α, β, and γ obtained indicate that $CaCu_3Ge_4O_{12}$ is a 3D coupled Ising ferromagnet with a small coercivity.

PACS numbers: 75.40.Cx, 75.47.Lx, 75.30.Et, 75.10.Hk

$CaCu_3Ge_4O_{12}$ crystallizes in an A-site 1:3 ordered cubic perovskite $AA'_3B_4O_{12}$ with $Im\bar{3}$ symmetry.[1] Fig.1(a) shows the crystal structure of $CaCu_3Ge_4O_{12}$ by highlighting the rotations of the cornered-shared $GeO_{6/2}$ octahedra. In this $2a_p \times 2a_p \times 2a_p$ cubic unit cell, the corner-shared $GeO_{6/2}$ octahedra are heavily tilted which leads to an average <Ge-O-Ge> bond angle of ~ 146°. This tilting is induced by the reduction of the 12-fold oxygen coordination of an A site occupied by a Cu^{2+} ion; a Cu^{2+} ion is stabilized in a square-coplanar CuO_4 coordination. The CuO_4 planes are oriented orthogonal to one another as is illustrated in Fig.1(b). In contrast to most magnetic transition-metal perovskites, the dominant interatomic exchange interactions are between magnetic ions on A sites in $CaCu_3Ge_4O_{12}$. Among the A-site-order perovskites $CaCu_3B_4O_{12}$, magnetic interactions between Cu^{2+} spins depend sensitively on the B-site cation.[2] Metallic Paramagnetism has been found in the compound with B = V,[3] Co,[4] and Ru [5] in which a heavy-Fermion state has been observed. The magnetic structures are complicated when the B-site cation contains localized magnetic moments such as Mn^{4+} [6] and Fe^{4+} [7]. But for non-magnetic B-site cations Ti,[1] Pt,[8] Ge,[1] and Sn [1], spin ordering on the A-site Cu^{2+} is antiferromagnetic for B = Ti (T_N = 25 K) and B = Pt (T_N = 40 K), ferromagnetic for B = Ge (T_c = 13 K) and Sn (T_c = 10 K). It has been argued [1, 8] that the involvement of the Ti-$3d^0$ and Pt-e_g^0 empty orbitals produces the antiferromagentic Cu-O-B-O-Cu superexchange interactions. On the other hand, the superexchange interactions through the 100 ° Cu-O-Cu bond indicated in Fig1(a) dominates where the B-ion orbitals are fully occupied, *i.e.* for B = Ge^{4+} and Sn^{4+}. The unusual bonding configuration for magnetic Cu^{2+} on A sites motivates us to study the critical behavior associated with the ferromagnetic transition in $CaCu_3Ge_4O_{12}$.

Magnetic interactions between localized spins in a crystal can be generally described by the Hamiltonian $H = -2J\sum_{i,j}[aS_i^zS_j^z + b(S_i^xS_j^x + S_i^yS_j^y)]$. The Hamiltonian covers the isotropic Heisenberg model (a = b = 1), the anisotropic XY model (a = 0, b = 1), and the Ising model (a = 1, b = 0). Different critical exponents corresponding to these models have been derived theoretically.[9] In a real magnetic system, however, critical behaviors are influenced by the energy scale of the magnetic transition temperature relative to

characteristic energies like crystal-field splitting, single-ion anisotropy, and spin-orbit coupling, which makes a specific model more applicable. The Heisenberg model is more suitable for magnets with a higher transition temperature. However, the 3D Ising ferromagnet is rare in existing magnets since the spin degree of freedom is reduced. It is interesting that the critical behaviors of perovskite ferromagnet $CaCu_3Ge_4O_{12}$ with $T_c \approx$ 12 K can be well-described by a 3D Ising model.

As reported in the literature [1], polycrystalline $CaCu_3Ge_4O_{12}$ samples in this study were prepared under high pressure and high temperature (HPHT) with a Walker-type multianvil module (Rockland Research Corp.). The precursor for HPHT synthesis was first obtained by calcining a stoichiometric mixture of $CaCO_3$, CuO, and GeO_2 at 1000°C for 24h in air. After regrinding, the precursor was sealed in a platinum capsule that was subjected to HPHT treatment at 6 GPa and 1000°C for 30 min. Details about our sample assembly for HPHT synthesis can be found elsewhere.[10] Phase purity of the samples obtained was checked with powder x-ray diffraction (XRD) at room temperature with a Philips X'pert diffractometer (Cu Kα radiation). The XRD pattern recorded in the 2θ range 15-120° with a step size of 0.02° and a dwell time of 10 s has been refined in the cubic Im-3 (No. 204) space group with the Rietveld method and the FullProf program;[11] the refinement converged very well with reliability factors: R_p = 3.29%, R_{wp} = 4.23%, and χ^2 = 1.27. The obtained lattice parameter a = 7.2090(1) Å agrees well with that of 7.202 Å reported by Ozaki *et al.*,[12] but is slightly smaller than that of 7.26701(1) Å reported in Ref. 1. However, the magnetic properties of the present study are nearly identical to those reported in Ref. 1 as discussed below. We noticed that the XRD profile of our sample exhibits very sharp peaks close to the instrumental resolution. For example, the full width at half maximum (FWHM) of the main peak (220) at 2θ = 35.182° is 0.0768°, while the instrumental broadening determined from a LaB_6 standard at this angle is about 0.078°. Such a narrow diffraction profile indicates that the sample is not only well-crystallized, but also to have a high degree of ordering of Ca and Cu ions at the A sites. Magnetic properties and specific heat of the high-pressure products have been measured with a superconducting quantum interference device (SQUID) magnetometer (Quantum Design) and a Physical Properties Measurement System (PPMS, Quantum

Design), respectively. The temperature dependence of the magnetization M(T) measured under a magnetic field of H = 2000 Oe exhibits a sharp increase at low temperatures with a sharp minimum at T = 12.5 K in the temperature derivative of dM/dT; the high-temperature Curie-Weiss fitting yields μ_{eff} = 1.91 μ_B/Cu and θ_{cw} = 14.2 K. The M(H) curve between +5 and -5 T measured at 5 K gives a saturation moment of 1.1μ_B/Cu and a coercive force H_c smaller than 15 Oe. These results are consistent with those reported in ref. 1. In the following, we focus on the critical behaviors of $CaCu_3Ge_4O_{12}$ around T_c.

Fig. 2(a) shows the isothermal magnetization curves M vs H of $CaCu_3Ge_4O_{12}$ in the temperature range 9 –15 K, where the demagnetization effect has been corrected. Isotherms in the M^2 vs H/M plot, Fig. 2(b), are curved, which rules out the possibility to use a mean-field model. We have analyzed the magnetization by using the general formula for the critical exponents.

$$M(T) \sim |T/T_c-1|^{\beta}, \quad T < T_c \qquad (1)$$

$$\chi^{-1}(T) \sim |T/T_c-1|^{\gamma}, \quad T > T_c \qquad (2)$$

$$M(H) \sim H^{1/\delta}, \quad T = T_c \qquad (3)$$

Isotherms were plotted in Fig.2(c) – (d) in the modified Arrott plot $M^{1/\beta}$ versus $(H/M)^{1/\gamma}$ with the critical exponents of 3D Heisenberg (c) and 3D Ising (d) models. Although both the modified Arrott plots of the 3D Heisenberg and Ising models can produce roughly straight lines, a close inspection shows that the lines below and above T_c in the plot of 3D Ising model are more parallel than those in the plot of 3D Heisenberg model, which suggests that the ferromagnetism of $CaCu_3Ge_4O_{12}$ could be better described with the 3D Ising model.

This conjecture has been further refined through iterations of the modified Arrott plot and formula for the critical exponents; more precise critical exponents of β and γ were obtained after the iterations converge.[13,14] Fig. 3(a) illustrates results after three iterations. Critical exponents converged quickly to β = 0.317(5), γ = 1.18(2), and $T_c \approx$ 11.95 K. By using $M_s(T)$ and $\chi_0^{-1}(T)$ obtained by extrapolating an isotherm to either the vertical or the horizontal axes in the modified Arrott plot with the final critical exponents, we have checked the Kouvel-Fisher (KF) relation,[15] *viz.*

$$M_s(T)[dM_s(T)/dT]^{-1} = (T-T_c^-)/\beta, \quad (4)$$

$$\chi_0^{-1}(T)[d\chi_0^{-1}(T)/dT]^{-1} = (T-T_c^+)/\gamma. \quad (5)$$

Linear fittings to the plots of $M_s(T)[dM_s(T)/dT]^{-1}$ and $\chi_0^{-1}(T)[d\chi_0^{-1}(T)/dT]^{-1}$ versus T in Fig. 3(b) yield $\beta = 0.310(9)$ and $\gamma = 1.20(3)$. Both values of β and γ obtained by the KF relation are well consistent with results from the iterations of the Arrott plot and are very close to those of the 3D Ising model: $\beta = 0.325$ and $\gamma = 1.241$. We also obtained the critical exponent δ associated with the critical isotherm M(H) at T_c. The log-log plot of M vs H in Fig. 3(c) of the isotherm at $T_c = 12$ K fits a line with $\delta = 4.82(6)$. Critical exponents of $CaCu_3Ge_4O_{12}$ obtained in this study satisfy perfectly the Widom scaling relation,[16] $\delta = 1+ \gamma/\beta$. These critical exponents are listed in Table I together with those theoretical values from different models for comparison.

In order to test reliability of our analysis for the critical behavior in $CaCu_3Ge_4O_{12}$, isotherms have been plotted based on the scaling hypothesis: [9]

$$M(H, \varepsilon) = |\varepsilon|^{\beta} f_{\pm}(H/|\varepsilon|^{\beta+\gamma}), \quad (6)$$

where f_+ for $T > T_c$ and f_- for $T < T_c$ are regular analytical functions, and $\varepsilon = T/T_c-1$ is the reduced temperature. Equation (6) implies that the $M/|\varepsilon|^{\beta}$ as a function of $H/|\varepsilon|^{\beta+\gamma}$ produces two universal curves: one for $T < T_c$ and the other for $T > T_c$. By using the values of β and γ obtained by the KF method and $T_c = 11.95$ K, we have obtained the scaled data plotted in Fig. 4; all the points indeed fall on two curves. One may concern the residual strain effect on the critical behavior. To this end, we have checked the critical behavior from the $CaCu_3Ge_4O_{12}$ sample annealed at 200°C for 12 h in air in order to remove the residual strain created during HPHT synthesis. The sample exhibits the same critical behavior as that in the as-prepared sample.

A complete analysis of critical behavior should also include a thorough study of specific heat. By using the standard procedure in the PPMS, we obtained the $C_p(T)$ of $CaCu_3Ge_4O_{12}$ which is identical to that in the literature[1]. However, data as shown in Fig.5(a) collected with the finest temperature interval include limited information for tracking down the critical behavior near T_c. In order to overcome this difficulty, we have

made use of a larger heat pulse and collected data while the heat pulse decays over a temperature range across T_c.[17] The C_p data calculated from the pulse decay are shown in Fig.5(b) together with the C_p data of Ni [18] scaled at $T_c = 11.88$ K for comparison. The dramatic difference between two curves occurs at $T < T_c$. The C_p data have been analyzed with the power-law formula[19] for the critical behavior;

$$C_p^{+} = A^{+}(\varepsilon^{-\alpha^{+}} - 1)/\alpha^{+} + B^{+} + D^{+}\varepsilon, \quad T > T_c; \tag{7}$$

$$C_p^{-} = A^{-}(|\varepsilon|^{-\alpha^{-}} - 1)/\alpha^{-} + B^{-} + D^{-}\varepsilon, \quad T < T_c; \tag{8}$$

Whereas fitting to the C_p data of Ni gives an $\alpha = -0.087(3)$ for both C_p^{+} and C_p^{-}, characteristic of the 3D Heisenberg mode, the fitting quality with a single α for both C_p^{+} and C_p^{-} is poorer than that with two different αs for $CaCu_3Ge_4O_{12}$; all parameters for the best fitting are listed in Table II. Baker [20] has shown theoretically that the 3D Ising model specific heat becomes singular like $\log|\varepsilon|$ with a different coefficient above and below the singular point. Moreover, an $\alpha = 0.13(2)$ for C_p^{+} of $CaCu_3Ge_4O_{12}$ fits well the 3D Ising model.[9]

The most studied Ising system is the magnetic dipolar ferromagnet $LiTbF_4$,[21] where week long-range dipole-dipole interactions dominate. The exchange interactions and an unquenched orbital angular momentum are strongly coupled to the lattice. It is, therefore, surprising that the critical behaviors of the perovskite $CaCu_3Ge_4O_{12}$ can be described by a 3D Ising model since the orbital angular momentum of square-coplanar Cu^{2+} is quenched to first-order and the small coercivity signals a weak coupling of the spins to the lattice. Although there is no first-order orbital angular momentum on the Cu^{2+} ion, the single e_g hole is ordered into the CuO_4 planes to give a site anisotropy that would order the spins perpendicular to a CuO_4 plane. But neighboring CuO_4 planes are orthogonal to one another, which gives a frustrated easy spin axis for spins aligned collinearly by a ferromagnetic 100° Cu-O-Cu superexchange interaction. A neutron-diffraction study [22] of antiferromagnetic, isostructural $CaCu_3Ti_4O_{12}$ has indicated the spins are oriented along a $\langle 111 \rangle$ axis, so we assume that a $\langle 111 \rangle$ easy axis is also the compromise for the site

anisotropies of $CaCu_3Ge_4O_{12}$. This compromise would give strong coupling of the spins to a ⟨111⟩ direction, but would allow easy switching between ⟨111⟩ directions to give a low coercive force H_c. We believe it is the frustration of the site easy axes in the presence of a strong interatomic exchange interaction that is responsible for Ising critical fluctuations in a ferromagnet with small coercivity.

In conclusion, we have carried out a comprehensive study of the critical behavior associated with the ferromagnetic transition in the 1: 3 A-site-perovskite $CaCu_3Ge_4O_{12}$ from the isothermal magnetization data and specific heat in the vicinity of $T_c \approx 12$ K. The critical exponents $\beta \approx 0.32$ and $\gamma \approx 1.20$, and $\alpha \approx 0.13$ for C_p^+ obtained suggest that $CaCu_3Ge_4O_{12}$ is an extremely rare example of a 3D Ising ferromagnet having a small coercivity.

Acknowledgements

This work was supported by NSF (DMR 0904282, CBET 1048767) and the Robert A Welch foundation (Grant F-1066).

jszhou@mail.utexas.edu

Table 1 Critical exponents of $CaCu_3Ge_4O_{12}$ and theoretical values from three models.

	Ref.	α	β	γ	δ
$CaCu_3Ge_4O_{12}$	This work	0.13(2)	0.320(9)	1.20(3)	4.82(6)
Mean-field model	9	0	0.5	1.0	3.0
3D Heisenberg model	9	-0.10	0.365	1.386	4.80
3D Ising model	9	0.125	0.325	1.241	4.82

Table II Fitting parameters in equations (7) and (8) of the specific heat.

	log|ε|	α	T_c (K)	A	B	D
$T < T_c$	(-2.46, -1.03)	-0.03(7)	11.883(7)	3.6(9)	19.6(1.9)	28.8(4.6)
$T > T_c$	(-3.03, -1.0)	0.13(2)	11.881(1)	2.15(23)	6.2(7)	-19.8(2.7)

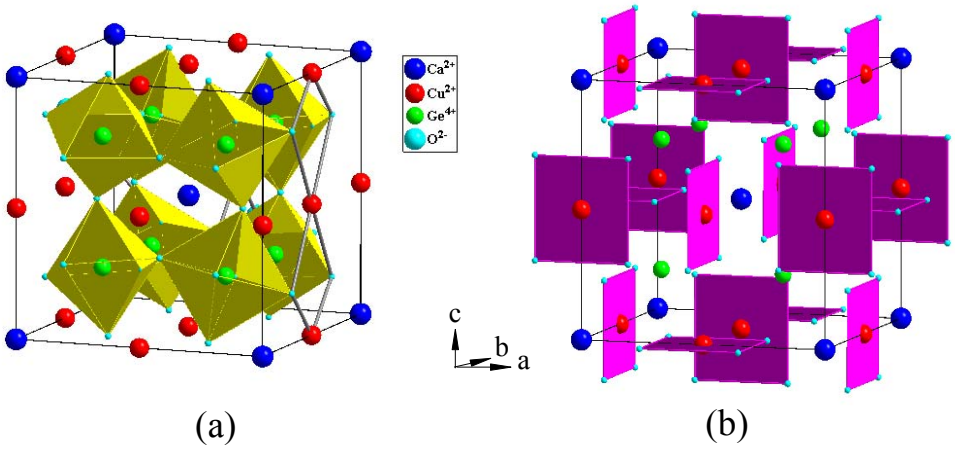

Fig. 1 (Color Online) Crystal structure of $CaCu_3Ge_4O_{12}$ by highlighting (a) the network of corner-shared $GeO_{6/2}$ octahedra and the superexchange interatomic interaction through the 100° Cu-O-Cu bond and (b) the perpendicular alignment of the CuO_4 planes.

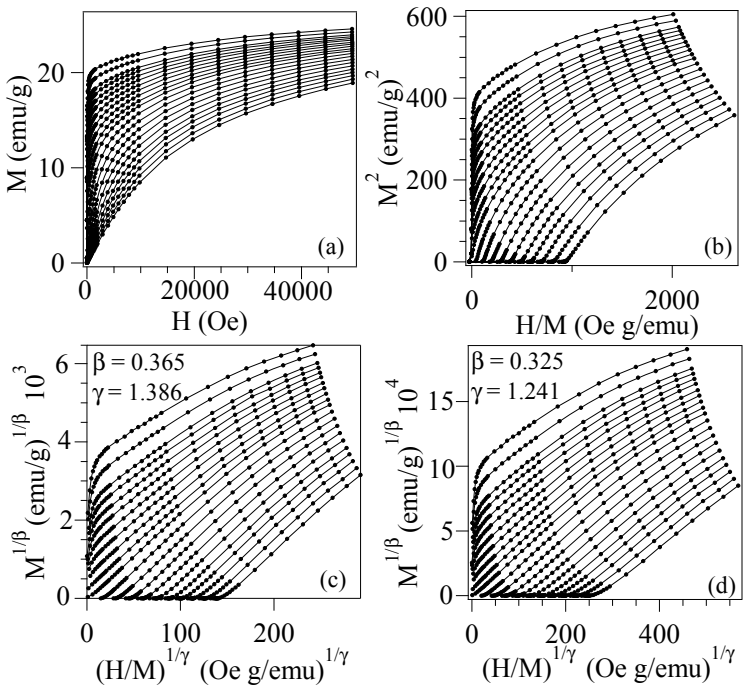

Fig. 2 (a) Isothermal magnetization curves between 9 K and 15 K, and the modified Arrott plots with critical exponents of (b) mean-field model, (c) 3D Heisenberg model, and (d) 3D Ising model.

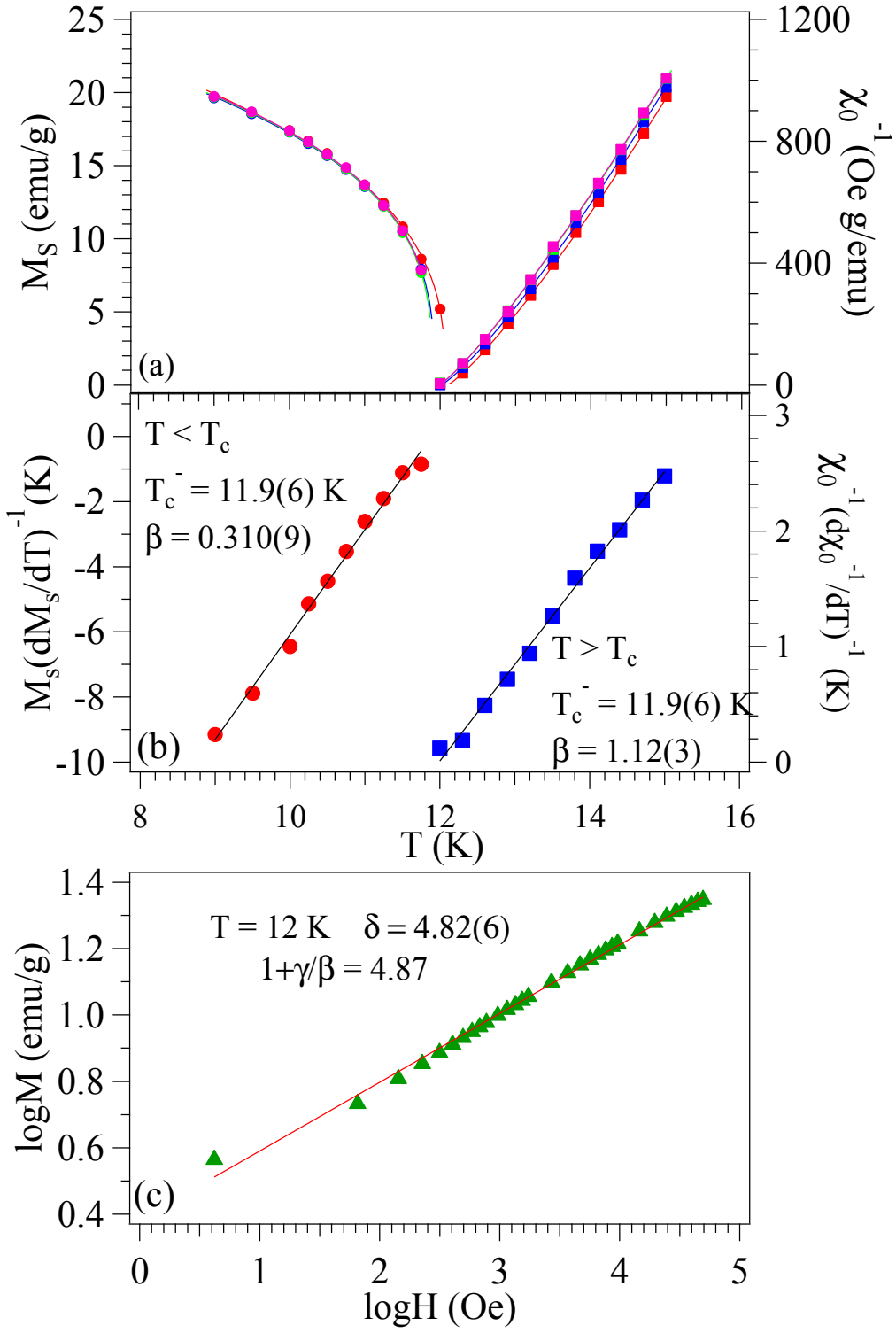

Fig. 3 (Color Online) Critical exponents, β and γ, and critical temperatures, T_c^- and T_c^+, determined from (a) an iteration process started from the mean-field Arrott plot, and (b)

Kouvel-Fisher plots. (c) Critical isotherms at T = 12 K and the fulfillment of the Widom Scaling relation:[16] $\delta = 1 + \gamma/\beta$.

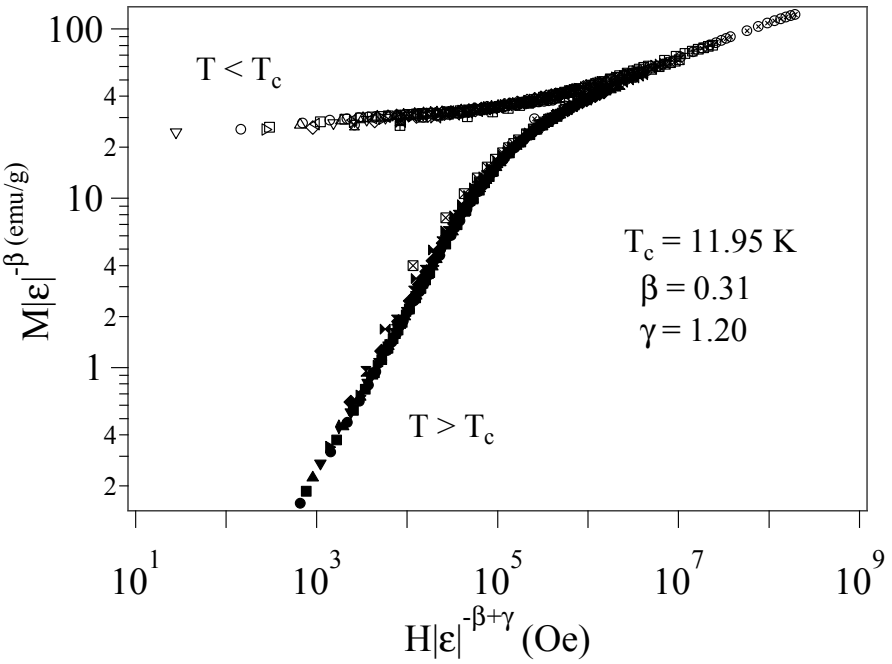

Fig. 4 Scaling plot for $CaCu_3Ge_4O_{12}$ below and above T_c based on the critical temperature T_c = 11.95 K and critical exponents β = 0.310 and γ = 1.20.

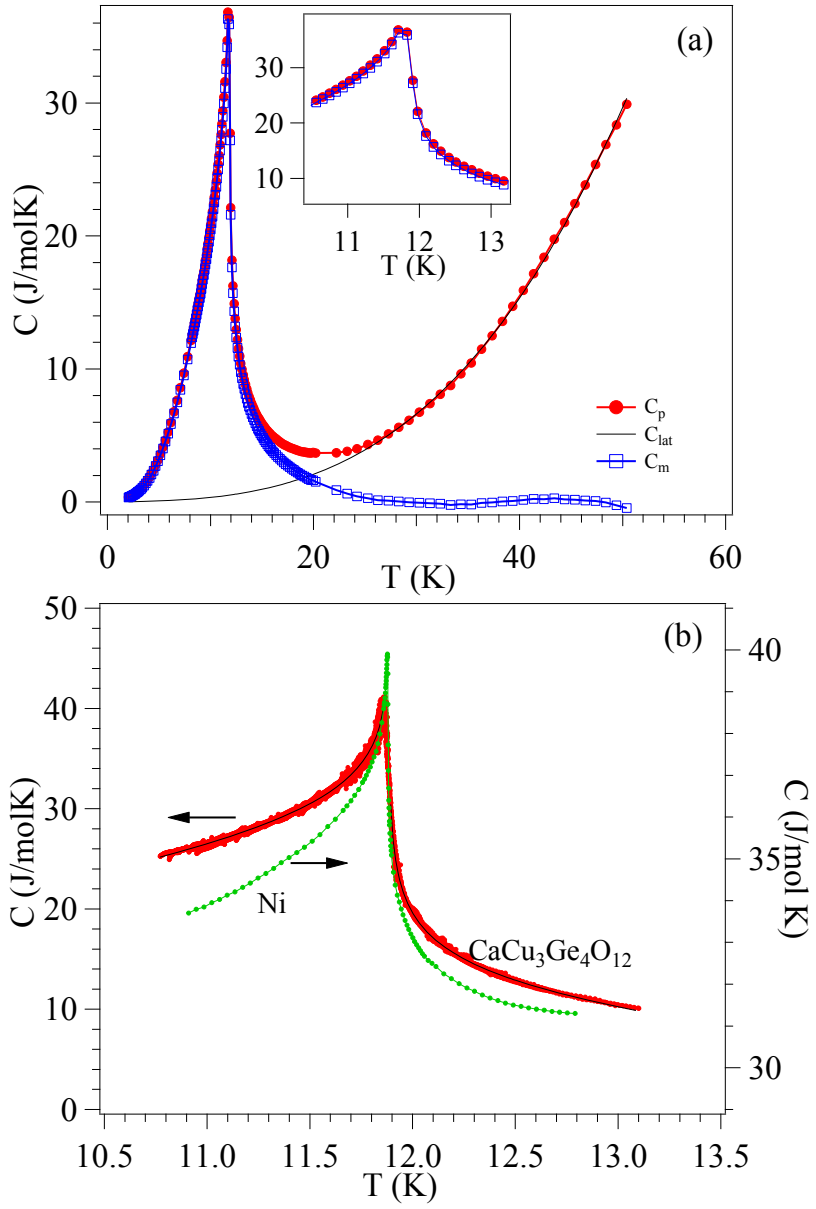

Fig. 5 (color online) Temperature dependence of specific heat of $CaCu_3Ge_4O_{12}$ (a) result obtained with the standard procedure for the C_p measurement in a PPMS; (b) result derived from the temperature profile during the pulse decays.[17] The C_p data of Ni are from ref. 18.

[1] H. Shiraki, T. Saito, T. Yamada, M. Tsujimoto, M. Azuma, H. Kurata, S. Isoda, M. Takano, and Y. Shimakawa, Phys. Rev. B **76**, 140403 (2007).

[2] Y. Shimakawa, Inorg. Chem. **47**, 8562 (2008).

[3] H. Shiraki, T. Saito, M. Azuma, and Y. Shimakawa, J. Phys. Soc. Jpn. **77**, 064705 (2008).

[4] T. Mizokawa, Y. Morita, T. Sudayama, K. Takubo, I. Yamada, M. Azuma, M. Takano, and Y. Shimakawa, Phys. Rev. B **80**, 125105 (2009).

[5] S. Tanaka, N. Shimazui, H. Takatsu, S. Yonezawa, and Y. Maeno, J. Phys. Soc. Jpn. **78**, 024706 (2009).

[6] J. Sánchez-Benítez, J. A. Alonso, M. J. Martínez-Lope, M. T. Casais, J. L. Martínez, A. de Andrés, and M. T. Fernández-Díaz, Chem. Mater. **15**, 2193 (2003).

[7] I. Yamada, K. Takata, N. Hayashi, S. Shinohara, M. Azuma, S. Mori, S. Muranaka, Y. Shimakawa, and M. Takano, Angew. Chem. Int. Ed. **47**, 7032 (2008).

[8] I. Yamada, Y. Takahashi, K. Ohgushi, N. Nishiyama, R. Takahashi, K. Wada, T. Kunimoto, H. Ohfuji, Y. Kojima, T. Inoue, and T. Irifune, Inorg. Chem. **49**, 6778 (2010).

[9] H. E. Stanley, *Introduction to Phase Transition and Critical Phenomena* (Oxford University Press, London, 1971)

[10] J.-G. Cheng, J.-S. Zhou, and J. B. Goodenough, Phys. Rev. B **81**, 134412 (2010).

[11] J. Rodriguez-Carvajal, Physica B **192**, 55 (1993).

[12] Y. Ozaki, M. Ghedira, J. Chenavas, J. C. Joubert, and M. Marezio, Acta Cryst. **B 33**, 3615 (1977).

[13] F. Y. Yang, C. L. Chien, X. W. Li, G. Xiao, and A. Gupta, Phys. Rev. B **63**, 092403 (2001).

[14] H. Yanagihara, W. Cheong, M. B. Salamon, Sh. Xu, and Y. Moritomo, Phys. Rev. B **65**, 092411 (2002).

[15] J. S. Kouvel and M. E. Fisher, Phys. Rev. **136**, A1626 (1964).

[16] B. Widom, J. Chem. Phys. **41**, 1633 (1964).

[17] J. C. Lashley, M. F. Hundley, A. Migliori, J. L. Sarrao, P. G. Pagliuso, T. W. Darling, M. Jaime, J. C. Cooley, W. L. Hults, L. Morales, D. J. Thoma, J. L. Smith, J. Boerio-Goates, B. F. Woodfield, G. R. Stewart, R. A. Fisher, and N. E. Philips, Cryogenics **43**, 369 (2003).

[18] D. L. Connelly, J. S. Loomis, and D. E. Mapother, Phys. Rev. B **3**, 924 (1971).

[19] L. W. Shacklette , Phys. Rev. B **9**, 3789 (1974).

[20] G. A. Baker, Jr., Phys. Rev. **129**, 99 (1963).

[21] L. M. Holmes, J. Als-Nielsen, and H. J. Guggenheim, Phys. Rev. B **12**, 180 (1975); J. Als-Nielsen, L. M. Holmes, F. Krebs Larsen, and H. J. Guggenheim, Phys. Rev. B **12**, 191 (1975); J. Als-Nielsen, L. M. Holmes, and H. J. Guggenheim, Phys. Rev. Lett. **32**, 610 (1974).

[22] Y. J. Kim, S. Wakimoto, S. M. Shapiro, P. M. Gehring, and A. P. Ramirez, Solid State Commun. **121**, 625 (2002).